

Article

Amphiphilic Copolymer of Polyhedral Oligomeric Silsesquioxane (POSS) Methacrylate for Solid Dispersion of Paclitaxel

Suchismita Chatterjee  and Tooru Ooya * 

Graduate School of Engineering, Department of Chemical Science and Engineering, Kobe University, Kobe 657-8501, Japan; suchismita@stu.kobe-u.ac.jp

* Correspondence: ooya@tiger.kobe-u.ac.jp; Tel.: +81-78-803-6255

Received: 21 February 2019; Accepted: 27 March 2019; Published: 30 March 2019



Abstract: Suitable polymers for the homogeneous formulation of drug/polymer mixtures should be selected to correct the structural and physicochemical nature with a rapid dissolution rate. This study aimed to evaluate a copolymer prepared by the radical polymerization of 2-methacryloyloxyethyl phosphorylcholine (MPC) and a polyhedral oligomeric silsesquioxane (POSS) methacrylate bearing an ethyl (C₂H₅) group (MPC-*ran*-C₂H₅-POSS) as a carrier for the solid formulation of paclitaxel (PTX). A single-phase homogeneous formulation of PTX with the mixture of the MPC-*ran*-C₂H₅-POSS and polyvinylpyrrolidone (PVP) was prepared by a solvent method. The formulation of MPC-*ran*-C₂H₅-POSS/PVP/PTX enhanced the dissolution rate and the dissolved amount (approximately 90% within 40 min) without precipitation. The X-ray diffraction (XRD), Fourier transform infrared spectroscopy (FT-IR) and differential scanning calorimetry (DSC) analysis confirmed the presence of PTX as an amorphous state. The amphiphilic nature of the MPC-*ran*-C₂H₅-POSS contributed to enhancing the aqueous solubility of PTX. The new formulation is applicable for solid dispersion technique via the supersaturation of PTX in an aqueous media.

Keywords: 2-methacryloyloxyethyl phosphorylcholine (MPC); polyhedral oligomeric silsesquioxane (POSS); polyvinylpyrrolidone (PVP); paclitaxel; solid dispersion; dissolution

1. Introduction

Paclitaxel (PTX) is well known as an excellent clinical agent against various types of cancer such as breast, ovarian, stomach and lung cancers, etc. Due to the hydrophobic nature and low aqueous solubility (~0.4 µg/mL), PTX is incorporated in a mixture of Cremophor EL (polyoxyethylated castor oil) and dehydrated ethanol for intravenous administration. However, the solvent is known to cause a serious hypersensitivity reaction [1]. In order to improve this serious problem, various formulations of PTX have been investigated using biocompatible materials and different methods of administration. Solid dispersion technology using biocompatible materials has been extensively studied to improve the solubility and dissolution of poorly soluble drugs, including PTX [2,3]. For example, PTX was incorporated into poly(ϵ -caprolactone)-based film [4]. A PTX-encapsulated liposome was investigated to improve its aqueous solubility, stability and clinical efficacy [5,6]. Nanoplatfoms including nanoparticles (Abraxane[®]) and micelles (Genexol[®], Nanoxel[®] and Paclical[®]) have been used in clinical studies [7,8]. Alternatively, cyclodextrin complexes have been reported as formulations to increase water solubility [9,10], which has contributed to a decrease in toxicity. However, promising clinical effects have not yet been achieved.

Oral administration of PTX is important for the successful implementation of low-dose metronomic (LDM) chemotherapy, where relatively low doses of the drug are frequently administered with no

drug-free periods, in terms of patient convenience and compliance. The major limitation of oral administration is the poor aqueous solubility of PTX, leading to poor bioavailability [11]. Recent studies suggest that a PTX-loaded glycyrrhizic acid (GA) micelle improved the oral bioavailability of PTX [12]. From the viewpoint of developing solid dispersion, suitable polymers to prepare the best solid dispersion should be designed depending on the chemical structure of poorly soluble drugs. For example, a copolymer composed of a 2-methacryloyloxyethyl phosphorylcholine (MPC) unit and a butyl methacrylate (BMA) unit (poly[MPC-co-BMA]) has been prepared [13], and the polymer spontaneously formed a micelle-like structure in an aqueous condition, where the hydrophobic domain could hydrophobically interact with PTX to solubilize it [14]. The poly[MPC-co-BMA] was also applied for the solid dispersion of tranilast (*N*-(3,4-dimethoxycinnamoyl) anthranilic acid), an anti-allergic biopharmaceutics classification system (BSC) class II drug [15]. The poly[MPC-co-BMA] markedly improved the dissolution rate by the attractive interaction between the polymer and tranilast. Historically, polyvinylpyrrolidone (PVP) has been extensively used for solid dispersions to improve the dissolution rate without recrystallization due to the enhanced interaction in the solid state [16]. A solid dispersion containing PVP, sodium lauryl sulfate (SLS) and PTX is a good strategy for increasing the solubility and dissolution rate of PTX, with the solid dispersion formulation of PTX having been tried with the first clinical trial using oral LDM chemotherapy [11]. According to a literature review, the design of water-soluble polymers, which preferably interact with PTX to keep the amorphous states, should be considered as a crucial factor to improve the solubility and dissolution rate of PTX [17].

Based on those perspectives of the MPC-based amphiphilic copolymers, this study focused on the MPC as a hydrophilic monomer as well as the chemical structure of hydrophobic monomers, because the BMA part of poly[MPC-co-BMA] as mentioned above is not optimized for controlling the interaction with PTX. In a previous study, a random copolymer was synthesized by using the MPC and ethyl (C_2H_5) group-modified polyhedral oligomeric silsesquioxane (POSS) methacrylate (MA) as a hydrophobic monomer [18]. The obtained copolymer (MPC-*ran*- C_2H_5 -POSS; Figure 1a) was not cytotoxic [18], and it formed a hydrophobic domain in water through the hydrophobic interaction of the C_2H_5 -POSS moiety. In addition, it was found that the tight interaction between the C_2H_5 -POSS and PTX was correlated with the slow release of PTX from a micelle-like assembly of MPC-*ran*- C_2H_5 -POSS [19]. Thus, the MPC-*ran*- C_2H_5 -POSS solubilizes PTX well, and this finding led to the idea of the application of the MPC-*ran*- C_2H_5 -POSS for a homogeneous solid formulation. In this study, the MPC-*ran*- C_2H_5 -POSS was investigated as a potential carrier of PTX in the formulation of a drug/polymer mixture. The solid formulation of PTX and the MPC-*ran*- C_2H_5 -POSS was prepared by a simple evaporation method. PVP (Figure 1b) was also added to the MPC-*ran*- C_2H_5 -POSS as an additional hydrophilic carrier to evaluate the role of PVP in the MPC-*ran*- C_2H_5 -POSS matrix. The solid states of PTX in the polymeric matrix were characterized by X-ray diffraction (XRD), Fourier transform infrared spectroscopy (FT-IR) and differential scanning calorimetry (DSC). The PTX dissolution behavior from the formulations was investigated and the effect of the MPC-*ran*- C_2H_5 -POSS on the PTX dissolution was discussed. The enhanced dissolution of PTX was found without any precipitation, which was correlated with maintaining the amorphous nature of PTX in the MPC-*ran*- C_2H_5 -POSS/PVP matrix.

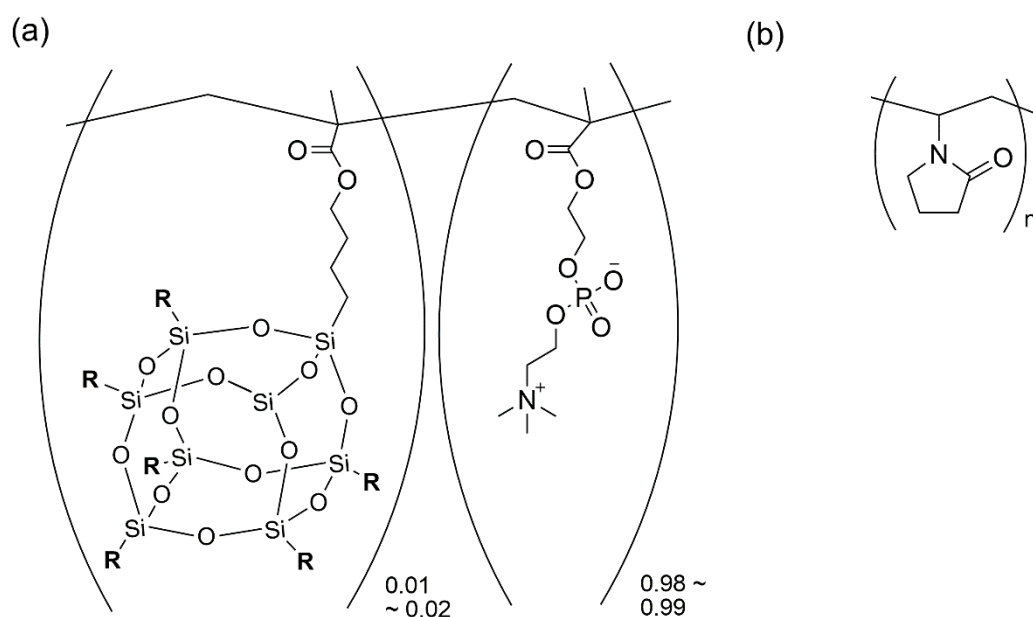


Figure 1. Chemical structure of (a) 2-methacryloyloxyethyl phosphorylcholine (MPC) and a polyhedral oligomeric silsesquioxane (POSS) methacrylate bearing an ethyl (C_2H_5) group (MPC-*ran*- C_2H_5 -POSS) ($R = C_2H_5$) and (b) polyvinylpyrrolidone (PVP).

2. Materials and Methods

2.1. Materials

The 2-methacryloyloxyethyl phosphorylcholine (MPC) was purchased from NOF Corporation (Tokyo, Japan). The MPC-*ran*- C_2H_5 -POSS copolymer was synthesized using a previously described method (Figure S1 in Supplementary Materials) [18]. The mol. % of C_2H_5 -POSS in the copolymer was found to be ca. 2 mol. %, which was calculated by the 1H NMR spectrum (Figure S2 in Supplementary Materials). PTX and 2nd Fluid for dissolution test were purchased from FUJIFILM Wako Pure Chemical Corporation, Osaka, Japan. PVP K30 ($M_n = 50,000$) was purchased from Sigma-Aldrich Co. LLC. (St. Louis, MO, U.S.A.). The other reagents and solvents were used without further purification.

2.2. PTX Solid Formulation Using MPC-*ran*- C_2H_5 -POSS and PVP

The formulation of MPC-*ran*- C_2H_5 -POSS, PVP and PTX (MPC-*ran*- C_2H_5 -POSS/PVP/PTX) was prepared using a solvent method. The MPC-*ran*- C_2H_5 -POSS, PVP and PTX were dissolved in dehydrated ethanol (MPC-*ran*- C_2H_5 -POSS:PVP:PTX = 44:44:12 wt. %) with continuous stirring. The solvent was removed under vacuum at room temperature. The MPC-*ran*- C_2H_5 -POSS/PTX (C_2H_5 -POSS-MA MPC:PTX = 88:12 wt. %) and the PTX/PVP (PVP:PTX = 88:12 wt. %) were also prepared in the same manner.

2.3. Dissolution Test

The dissolution of the solid formulation was tested according to the European Pharmacopoeia, using a type 2 (paddle) dissolution apparatus (NTR-6100A, Toyama Sangyo Co., Ltd., Osaka, Japan). The dissolution study was performed in 500 mL of 2nd Fluid for dissolution test mixed with 1% Tween 80 as a dissolution medium. The temperature was kept at 37 °C during the study with a stirring speed of 100 rpm. The solid dose form of 10 mg was used in this dissolution study, which contained 1.1 mg equivalent of PTX. The sample solutions (25 mL) were collected at 5, 10, 20, 30, 40, 50, 60, 90, 120 and 180 min time points and an equivalent amount of fresh media was added to maintain a constant dissolution volume. The concentration of PTX in the dissolution medium was determined by HPLC (GILSON, Middleton, WI, U.S.A.) equipped with a UV-vis detector (Gilson 119 UV/VIS

Detector, GILSON, Middleton, WI, U.S.A.), two pumps (GILSON 805 Manometric Module and 306 Pump, GILSON, Middleton, WI, U.S.A.), a mixer (GILSON 811c dynamic mixer, GILSON, Middleton, WI, U.S.A.) and a column (TSKgel ODS-100S (Φ 4.6 nm \times 150 mm)) from TOSOH Co., Tokyo, Japan). Before the measurements were taken, all the samples were filtered through 0.45 μ m Polyvinylidene difluoride (PVDF) membrane filters. A methanol and water (70:30 v/v) mixed solution was used as the mobile phase, and a 1 mL/min flow rate was maintained during the measurements. The detection was performed at a wavelength of 227 nm. PTX release in the dissolution medium at different time intervals was calculated using the PTX standard curve. The standard solutions of concentrations 100, 50, 10, 1 and 0.1 μ g/mL were prepared in methanol and the standard curve was prepared by plotting the area under the peak vs. concentration. The resulting standard curve was linear with $R^2 = 0.9949$. All the dissolution experiments were conducted in triplicate.

2.4. X-Ray Diffraction (XRD)

Powder X-ray diffraction was carried out using an X-Ray diffractometer (RINT2000, Rigaku Co., Tokyo, Japan) with monochromatic $\text{CuK}\alpha$ radiation and a generator working at 40 kV and 20 mA. Scattering intensity was measured in the range of $2 < 2\theta < 60^\circ$ with scan steps of 1° min^{-1} .

2.5. Fourier Transform Infrared Spectroscopy (FT-IR)

The chemical bonds of the solid formulation were characterized using a Fourier transform infrared spectroscopy (FT-IR) apparatus (JASCO FT/IR-460plus, JASCO Corporation, Tokyo, Japan). The scanning wave numbers ranged from 4000 to 400 cm^{-1} . KBr was used for the attenuated total reflectance crystal. The spectra were recorded from KBr pellets, prepared by mixing the formulation with KBr at room temperature. The spectrum resolution was 4 cm^{-1} , and 2 mm s^{-1} scans were accumulated to determine one spectrum.

2.6. Differential Scanning Calorimetry (DSC)

Thermal analyses of the formulation were carried out using a differential scanning calorimetry (DSC) apparatus (EXSTAR 6000/DSC6200, Seiko Instruments Inc., Chiba, Japan). The scan rate was $10^\circ \text{C min}^{-1}$ (first cooling, second cooling, first heating and second heating) within the temperature range of 20–185 $^\circ\text{C}$. The glass transition temperature (T_g) was obtained at the midpoint of change in the baseline of DSC thermograms during the second heating. The T_g of the solid formulation ($T_{g \text{ mix}}$) was calculated by using the Fox equation [11],

$$1/T_{g \text{ mix}} = \sum_i w_i/T_{g i} \quad (1)$$

where w_i is the weight fraction of the i^{th} pure component and $T_{g i}$ is the glass transition temperature (in Kelvin) of the i^{th} pure component.

3. Results and Discussion

3.1. Characterization of the PTX Solid Formulation

Three different formulations of PTX were prepared in this study at the same weight percentage of PTX in all the formulations: MPC-*ran*- C_2H_5 -POSS:PVP:PTX = 44:44:12 wt. % (MPC-*ran*- C_2H_5 -POSS/PVP/PTX), MPC-*ran*- C_2H_5 -POSS:PTX = 88:12 wt. % (MPC-*ran*- C_2H_5 -POSS/PTX) and PVP:PTX = 88:12 wt. % (PVP/PTX). In order to characterize the crystalline and amorphous states of PTX and polymers in those solid formulations, XRD, DSC and FT-IR measurements were carried out.

XRD spectra of the MPC-*ran*- C_2H_5 -POSS, PVP, PTX and the three different formulations are shown in Figure 2a. The semi-crystalline PTX showed diffraction peaks at 5.5° , 8.7° and 12.6° as shown in Figure 2a-C, which was consistent with the previous report [20]. The characteristic

peaks of PTX as seen in Figure 2a-C were not observed in the MPC-*ran*-C₂H₅-POSS/PTX, PVP/PTX or the MPC-*ran*-C₂H₅-POSS/PVP/PTX formulations (Figure 2a-D,E,F), suggesting that the PTX existed as an amorphous state in those formulations. This finding is consistent with previous reports of PTX solid dispersion [4]. This result indicates that PTX was finely distributed over the MPC-*ran*-C₂H₅-POSS/PVP/PTX in the solid homogeneous matrix [11,21].

From the DSC thermograms (Figure 2b and Figure S3 in the Supplementary Materials), T_g of the solid formulations and the constituent polymers were calculated, and the results supported the results of the XRD. The T_g of MPC-*ran*-C₂H₅-POSS, PVP and PTX were observed at 70 °C (343 K), 156 °C (429 K) and 106 °C (379 K), respectively. The detailed calculation of T_g is shown in Figure S3-A-C in the Supplementary Materials. Since the obtained T_g of PVP was consistent with the findings of a previous study [22], the calculation of T_g values from the second heating curves was reliable. It is known that PTX exhibits a melting point at 213–217 °C as a semi-crystal [23]. However, it also bears a T_g in an amorphous state [24]. The MPC-*ran*-C₂H₅-POSS/PVP/PTX solid formulation showed a single T_g at 91 °C (364 K) (Figure 2b-F and Figure S3-F in Supplementary Materials).

According to the Fox equation (Equation (1)), $T_{g\text{ mix}}$ of the MPC-*ran*-C₂H₅-POSS/PVP/PTX was calculated to be ca. 98 °C (381 K). Equation (1) only allows the prediction from the properties of pure components; the asymmetric entropic and enthalpic contribution are not reflected in this equation. In addition, the Equation (1) does not reflect the strength of intercomponent and intracomponent interaction, the composition-dependent energetic contribution from hetero-contact, the entropic effect, or the structural heterogeneity term. Taking the limitation of the Equation (1) into account, it is difficult to directly compare T_g with $T_{g\text{ mix}}$.

In the case of amorphous binary systems, the microstructure is closely related to the glass transition temperature, and the microstructural characteristics become evident in miscibility studies of binary polymer and drug/polymer mixtures (in this case, the MPC-*ran*-C₂H₅-POSS/PVP/PTX system) [25,26]. Brostow et al. proposed an analytical equation (the Brostow, Chiu, Kalogeras and Vassilikou-Dova (BCKV) equation) for predicting T_g that characterizes the binary systems as polymer blends or copolymers depending on their composition [26]:

$$T_g = \Delta T_g + x_1 T_{g1} + (1 - x_1) T_{g2} \quad (2)$$

$$\Delta T_g = x_1(1 - x_1) [a_0 + a_1(2x_1 - 1) + a_2(2x_1 - 1)^2] \quad (3)$$

where ΔT_g is the deviation from the linear function (the Fox equation), x_i is the mass fraction of component i and a_i represents the parameters of a polynomial (a quadratic polynomial for binary systems). In the proposed Equations (2) and (3), the parameters of a_i should be determined to correlate the experimental data. Moreover, they highlighted the complexity of such binary systems [26]. The high deviation between the experimental T_g values and the predicted values calculated by the Equation (1) is evidence of the increased complexity; the parameters of a_i in the equation reflect the differences between the strength of intercomponent and intracomponent interactions, composition-dependent energetic contributions from hetero-contacts, entropic effects and structural heterogeneities [25]. The BCKV equation was also used to correlate the experimental data from the investigation on the drug/polymer mixture, poly(vinyl pyrrolidone-*co*-vinyl acetate), and the results agreed well with the experimental data [27].

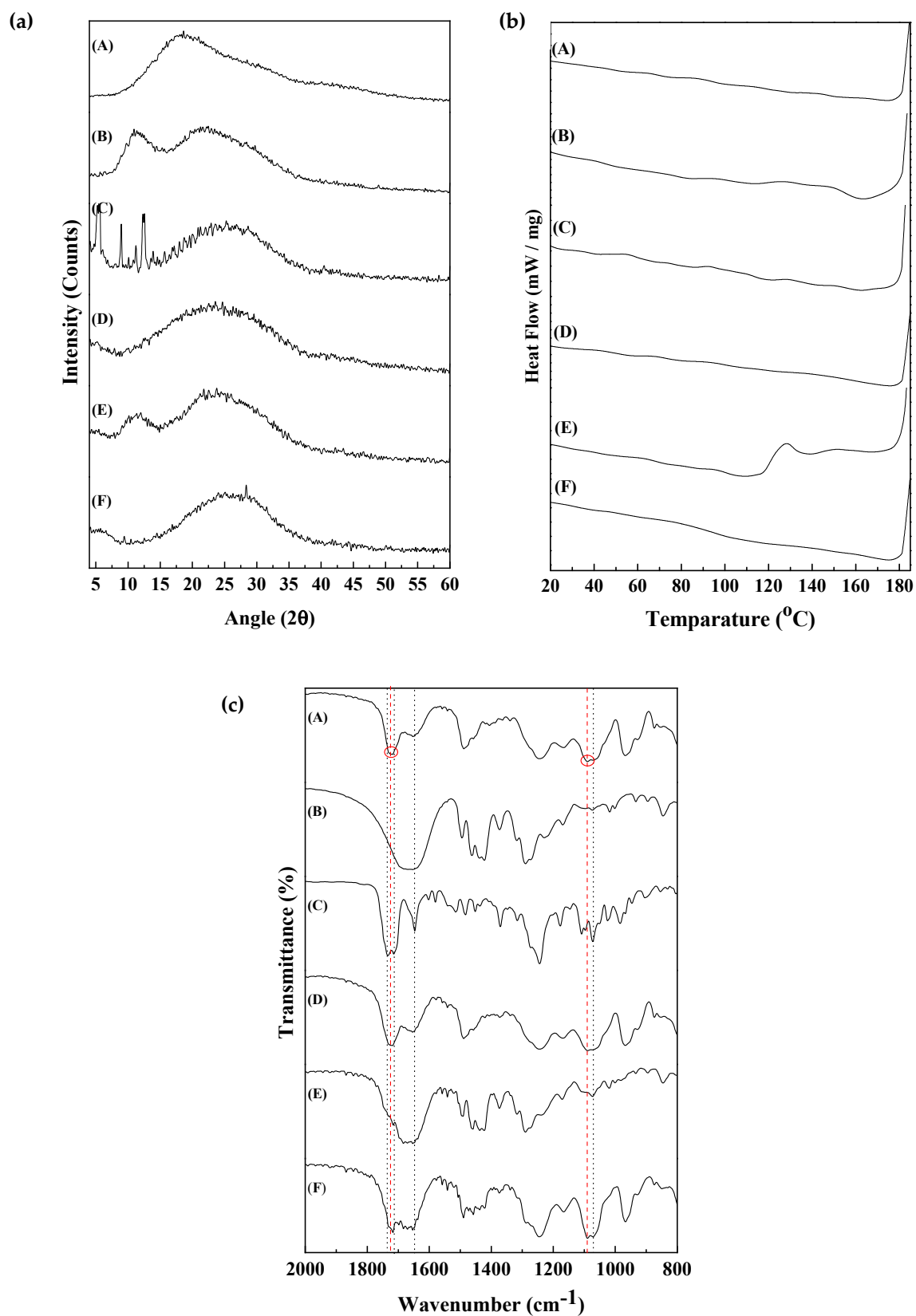


Figure 2. X-ray diffraction (XRD) spectra (a), differential scanning calorimetry (DSC) thermogram (b) and Fourier transform infrared spectroscopy (FT-IR) spectra (c) of A: MPC-*ran*-C₂H₅-POSS; B: PVP; C: paclitaxel (PTX); D: MPC-*ran*-C₂H₅-POSS/PTX; E: PVP/PTX; F: MPC-*ran*-C₂H₅-POSS/PVP/PTX.

According to the abovementioned perspectives of the complicated T_g estimation, the BCKV equation was applied to evaluate the formulation of the MPC-*ran*-C₂H₅-POSS/PVP/PTX. Table 1 shows the T_g values; the T_{gDSC} was determined by the DSC measurements (see Figure S3), and the $T_{g mix}$ was calculated by the Fox equation. The ΔT_g values, which were the difference between the T_{gDSC} and $T_{g mix}$ of the MPC-*ran*-C₂H₅-POSS/PTX, the PVP/PTX and the MPC-*ran*-C₂H₅-POSS/PVP/PTX, were -14 , -45 and -17 K, respectively. According to Equation (3), the ΔT_g values included the parameters of a_0 – a_2 (in the case of MPC-*ran*-C₂H₅-POSS/PVP/PTX, a_0 – a_3 due to the ternary systems). Since the parameters of a_i reflected the differences of the interaction energies and the structural heterogeneities as mentioned previously, those solid formulations exhibited some energetic matters of the interactions between the MPC-*ran*-C₂H₅-POSS, PVP and PTX. However, the smaller ΔT_g values of the MPC-*ran*-C₂H₅-POSS/PTX and the MPC-*ran*-C₂H₅-POSS/PVP/PTX compared to those of the PVP/PTX suggest that the MPC-*ran*-C₂H₅-POSS contributed to the increased miscibility of PTX.

Table 1. The glass transition temperature T_{gDSC} , the $T_{g mix}$ and the ΔT_g values of the formulations, the constituent polymers and PTX.

Sample Codes	T_{gDSC}^a (K)	$T_{g mix}^b$ (K)	$\Delta T_g (= T_{gDSC} - T_{g mix})$ (K)
MPC- <i>ran</i> -C ₂ H ₅ -POSS	343	-	-
PVP	429	-	-
PTX	379	-	-
MPC- <i>ran</i> -C ₂ H ₅ -POSS/PTX	333	347	-14
PVP/PTX	377	422	-45
MPC- <i>ran</i> -C ₂ H ₅ -POSS/PVP/PTX	364	381	-17

^a Experimentally determined T_g values from DSC data. ^b Calculated by Equation (1).

Since the T_g of the binary polymer and drug/polymer mixture is dependent on the mass fraction, the observed single T_g at 91 °C, which was higher than the value for the MPC-*ran*-C₂H₅-POSS (70 °C), follows conventional miscible organic blends [25]. In other words, the obtained single T_g value suggests the miscibility and strong interaction between PTX, PVP and polymers in the single homogeneous phase [11]. In addition, the increase of the T_g of the MPC-*ran*-C₂H₅-POSS (70 °C) to 91 °C suggests the increased stability of PTX by the strong interaction in the MPC-*ran*-C₂H₅-POSS/PVP/PTX homogeneous formulation [24].

From the FT-IR spectrum of PTX (Figure 2c-C), strong carbonyl bands were observed at 1715 cm⁻¹ (C=O, ketone) and 1734 cm⁻¹ ((C=O)-O-, ester) in addition to 1644 cm⁻¹ (aromatics) and 1070 cm⁻¹ (C-O-C). For the MPC-*ran*-C₂H₅-POSS, the corresponding ester bonds resulted in the appearance of the peaks at 1724 cm⁻¹ ((C=O)-O-, ester) and 1080 cm⁻¹ (P-O) in the MPC part [28] (Figure 2c-A). In the case of the MPC-*ran*-C₂H₅-POSS/PTX (Figure 2c-D), the similar spectrum of the MPC-*ran*-C₂H₅-POSS was observed. This suggested that the incorporated PTX in the MPC-*ran*-C₂H₅-POSS matrix was difficult to confirm from the IR spectrum; the FT-IR spectrum of the MPC-*ran*-C₂H₅-POSS/PTX was governed by the MPC-*ran*-C₂H₅-POSS. Besides, when PVP was added to the matrix (MPC-*ran*-C₂H₅-POSS/PVP/PTX), many jagged peaks around 1705–1740 cm⁻¹ were observed (Figure 2c-F). This suggests the restricted molecular interaction between individual components, which was consistent with the DSC data indicating a high $T_{g mix}$ of the solid formulation. This result also indicated that the PVP contributed to the reduction of crystallinity in the formulation. The FT-IR measurements of the physical mixture of the MPC-*ran*-C₂H₅-POSS/PTX, PVP/PTX and MPC-*ran*-C₂H₅-POSS/PVP/PTX were performed to confirm the detection of PTX in the FT-IR spectra; carbonyl bands at 1715 cm⁻¹ (C=O, ketone) and 1734 cm⁻¹ ((C=O)-O-, ester) in addition to 1644 cm⁻¹ (aromatics) and 1070 cm⁻¹ (C-O-C) at 12 wt. % (the same weight ratio; Figure S4 in the Supplementary Materials). The results of the FT-IR spectra of the physical mixture showed that the spectra were a summation of the individual components. The results suggest the negligible interactions between the components in combination. Thus, in the

formulation, PTX was more homogeneously distributed over the MPC-*ran*-C₂H₅-POSS/PVP matrix than in the physical mixture [11]. Taking all the information of XRD, DSC and FT-IR spectra into account, PTX existed as an amorphous state in the single phase homogeneous formulation.

3.2. Dissolution Behavior of PTX from the Formulation

Dissolution tests were carried out in order to assess the dissolution of PTX from the MPC-*ran*-C₂H₅-POSS/PVP/PTX, MPC-*ran*-C₂H₅-POSS/PTX and PVP/PTX. As shown in Figure 3, the dissolution rate of PTX from the MPC-*ran*-C₂H₅-POSS/PVP/PTX was much faster than that from the MPC-*ran*-C₂H₅-POSS/PTX and PVP/PTX for the first 10 min. Here, the dissolution rate was calculated from the slope of the first line curve between 0 to 10 min. The cumulative amount of PTX from the MPC-*ran*-C₂H₅-POSS/PVP/PTX was saturated until 20 min, and then the dissolution was accelerated. As a result, PTX was around 90% dissolved at 40 min. Since the complicated dissolution behavior was not observed in the case of the MPC-*ran*-C₂H₅-POSS/PTX and the PVP/PTX, the first stage of the dissolution up until 20 min was due to the synergistic effects of the MPC-*ran*-C₂H₅-POSS and PVP as the matrix. The second stage from 20 min to 40 min was governed by the MPC-*ran*-C₂H₅-POSS because the apparent dissolution behavior was similar to the MPC-*ran*-C₂H₅-POSS/PTX. The maximum PTX dissolution from the MPC-*ran*-C₂H₅-POSS/PVP/PTX was $\sim 2 \mu\text{g mL}^{-1}$ (an almost complete release of PTX) over 40 min. A similar phenomenon was observed in the case of the MPC-*ran*-C₂H₅-POSS/PTX, where the solubility of PTX was $\sim 1.5 \mu\text{g/mL}$. It is noted that the dissolved concentration percentage slowly decreased after reaching the maximum percentage. The general phenomenon of the homogeneous solid formulation was as follows—the decrease in the PTX concentration after a certain time was due to the fact that the crystal nucleation rate of PTX rises according to the ratio of the supersaturated solubility to the solubility of the crystal [29].

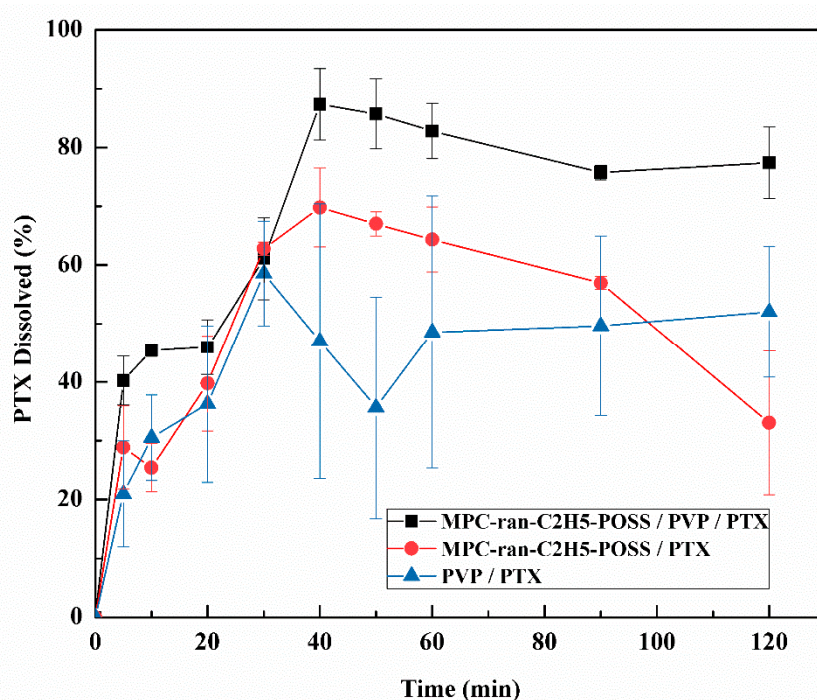


Figure 3. Dissolution profiles of PTX formulations in 2nd Fluid for dissolution test mixed with 1% Tween 80 at 37 °C; (■): MPC-*ran*-C₂H₅-POSS/PVP/PTX; (●): MPC-*ran*-C₂H₅-POSS/PTX; and (▲): PVP/PTX of solid formulations. Values are means \pm S.D. (n = 3).

The increase in the apparent dissolution from the MPC-*ran*-C₂H₅-POSS/PVP/PTX was caused by several factors such as the amorphous state of PTX in the formulations, Figure 2a-D,F, an enhanced solubilizing effect of the MPC-*ran*-C₂H₅-POSS (PTX solubility in the MPC-*ran*-C₂H₅-POSS 100 mg

mL⁻¹ solution was found to be $75.5 \pm 8.8 \mu\text{g}$) [19], the inhibited recrystallization of amorphous PTX by PVP and so on. Since the MPC-*ran*-C₂H₅-POSS exhibited an amphiphilic nature [19], the presence of the MPC-*ran*-C₂H₅-POSS could prevent the immediate recrystallization of amorphous PTX at the water interface to reduce interfacial tension between PTX and water [30]. In the case of the PVP/PTX, the amount of PTX dissolution was found to be lower than that in the MPC-*ran*-C₂H₅-POSS/PVP/PTX and the MPC-*ran*-C₂H₅-POSS/PTX, suggesting that the absence of hydrophobic moieties in the hydrophilic PVP matrix somewhat induced the recrystallization of PTX. Thus, the incorporation of the MPC-*ran*-C₂H₅-POSS in the solid formulation of PTX plays an important role in modulating the dissolution behavior of PTX, which leads to PTX supersaturation throughout the media [31].

4. Conclusions

MPC-*ran*-C₂H₅-POSS was incorporated into a solid formulation of PTX with PVP. The MPC-*ran*-C₂H₅-POSS/PVP/PTX single-phase homogeneous formulation was found to enhance the dissolution rate of PTX. The improved wetting of the formulation accompanied by the amphiphilic nature of the MPC-*ran*-C₂H₅-POSS facilitated rapid and complete drug release (approximately 90% within 40 min). The increased interaction between PTX and the polymeric matrix of the MPC-*ran*-C₂H₅-POSS/PVP/PTX formulation is likely to reduce the mobility of amorphous PTX, which results in the enhanced dissolution of PTX. Therefore, the formulation of PTX in combination with MPC-*ran*-C₂H₅-POSS and PVP would be a promising approach to enhance the physicochemical properties of PTX. The results obtained encourage further investigation of the pharmacokinetic parameters in an animal model.

Supplementary Materials: The following are available online at <http://www.mdpi.com/1996-1944/12/7/1058/s1>, Figure S1: Synthesis of MPC-*ran*-C₂H₅-POSS, Figure S2: A ¹H NMR spectrum of MPC-*ran*-C₂H₅-POSS in methanol-*d*₄, Figure S3: DSC thermograms of A: MPC-*ran*-C₂H₅-POSS; B: PVP; C: PTX; D: MPC-*ran*-C₂H₅-POSS/PTX; E: PVP/PTX; F: MPC-*ran*-C₂H₅-POSS/PVP/PTX, Figure S4: FT-IR spectra of A: PTX; B: MPC-*ran*-C₂H₅-POSS/PTX physical mixture; C: PVP/PTX physical mixture; D: MPC-*ran*-C₂H₅-POSS/PTX /PVP/PTX physical mixture.

Author Contributions: Conceptualization, T.O.; methodology, S.C. and T.O.; investigation, S.C.; writing—original draft preparation, S.C.; writing—review and editing, T.O.; supervision, T.O.; project administration, T.O.; funding acquisition, T.O.

Funding: This study was financially supported by a Grant-in-Aid for Scientific Research in Innovative Areas “New Polymeric Materials Based on Element-Blocks (No. 2401)” (JSPS KAKENHI grant number JP15H00748) and Izumi Science and Technology Foundation, Japan (2018-J-75). The authors would also like to thank the Toshimi Otsuka Scholarship Foundation for supporting the international student during this work.

Acknowledgments: We would like to thank Ayaka Kuroda (Kobe University) for help with the experiments of PTX solid dosage forms.

Conflicts of Interest: There are no conflicts of interest to declare.

References

1. Gelderblom, H.; Verweij, J.; Nooter, K.; Sparreboom, A. Cremophor EL: The drawbacks and advantages of vehicle selection for drug formulation. *Eur. J. Cancer* **2001**, *37*, 1590–1598. [[CrossRef](#)]
2. Alam, M.A.; Ali, R.; Al-Jenoobi, F.I.; Al-Mohizea, A.M. Solid dispersions: A strategy for poorly aqueous soluble drugs and technology updates. *Expert Opin. Drug Deliv.* **2012**, *9*, 1419–1440. [[CrossRef](#)]
3. Bikiaris, D.N. Solid dispersions, Part I: Recent evolutions and future opportunities in manufacturing methods for dissolution rate enhancement of poorly water-soluble drugs. *Expert Opin. Drug Deliv.* **2011**, *8*, 1501–1519. [[CrossRef](#)]
4. Shen, Y.Q.; Lu, F.; Hou, J.W.; Shen, Y.Y.; Guo, S.R. Incorporation of paclitaxel solid dispersions with poloxamer188 or polyethylene glycol to tune drug release from poly(epsilon-caprolactone) films. *Drug Dev. Ind. Pharm.* **2013**, *39*, 1187–1196. [[CrossRef](#)]
5. Yang, T.; Cui, F.D.; Choi, M.K.; Lin, H.X.; Chung, S.J.; Shim, C.K.; Kim, D.D. Liposome formulation of paclitaxel with enhanced solubility and stability. *Drug Deliv.* **2007**, *14*, 301–308. [[CrossRef](#)] [[PubMed](#)]

6. Hu, X.S.; Lin, L.; Xing, P.Y.; Zhang, C.G.; Wang, L.; Liz, Y.Q. The Clinical Efficacy and Safety of Paclitaxel Liposome on the Patients with Non-Small Cell Lung Cancer: A Meta-Analysis. *J. Thorac. Oncol.* **2017**, *12*, S902. [[CrossRef](#)]
7. Bernabeu, E.; Cagel, M.; Lagomarsino, E.; Moretton, M.; Chiappetta, D.A. Paclitaxel: What has been done and the challenges remain ahead. *Int. J. Pharm.* **2017**, *526*, 474–495. [[CrossRef](#)]
8. Louage, B.; De Wever, O.; Hennink, W.E.; De Geest, B.G. Developments and future clinical outlook of taxane nanomedicines. *J. Control. Release* **2017**, *253*, 137–152. [[CrossRef](#)]
9. Bouquet, W.; Ceelen, W.; Fritzing, B.; Pattyn, P.; Peeters, M.; Remon, J.P.; Vervaet, C. Paclitaxel/beta-cyclodextrin complexes for hyperthermic peritoneal perfusion—Formulation and stability. *Eur. J. Pharm. Biopharm.* **2007**, *66*, 391–397. [[CrossRef](#)]
10. Hamada, H.; Ishihara, K.; Masuoka, N.; Mikuni, K.; Nakajima, N. Enhancement of water-solubility and bioactivity of paclitaxel using modified cyclodextrins. *J. Biosci. Bioeng.* **2006**, *102*, 369–371. [[CrossRef](#)] [[PubMed](#)]
11. Moes, J.; Koolen, S.; Huitema, A.; Schellens, J.; Beijnen, J.; Nuijen, B. Development of an oral solid dispersion formulation for use in low-dose metronomic chemotherapy of paclitaxel. *Eur. J. Pharm. Biopharm.* **2013**, *83*, 87–94. [[CrossRef](#)]
12. Yang, F.H.; Zhang, Q.; Liang, Q.Y.; Wang, S.Q.; Zhao, B.X.; Wang, Y.T.; Cai, Y.; Li, G.F. Bioavailability Enhancement of Paclitaxel via a Novel Oral Drug Delivery System: Paclitaxel-Loaded Glycyrrhizic Acid Micelles. *Molecules* **2015**, *20*, 4337–4356. [[CrossRef](#)] [[PubMed](#)]
13. Yusa, S.I.; Fukuda, K.; Yamamoto, T.; Ishihara, K.; Morishima, Y. Synthesis of well-defined amphiphilic block copolymers having phospholipid polymer sequences as a novel biocompatible polymer micelle reagent. *Biomacromolecules* **2005**, *6*, 663–670. [[CrossRef](#)]
14. Konno, T.; Watanabe, J.; Ishihara, K. Enhanced solubility of paclitaxel using water-soluble and biocompatible 2-methacryloyloxyethyl phosphorylcholine polymers. *J. Biomed. Mater. Res. A* **2003**, *65*, 209–214. [[CrossRef](#)] [[PubMed](#)]
15. Onoue, S.; Kojo, Y.; Suzuki, H.; Yuminoki, K.; Kou, K.; Kawabata, Y.; Yamauchi, Y.; Hashimoto, N.; Yamada, S. Development of novel solid dispersion of tranilast using amphiphilic block copolymer for improved oral bioavailability. *Int. J. Pharm.* **2013**, *452*, 220–226. [[CrossRef](#)] [[PubMed](#)]
16. Taylor, L.S.; Zografi, G. Spectroscopic characterization of interactions between PVP and indomethacin in amorphous molecular dispersions. *Pharm. Res.* **1997**, *14*, 1691–1698. [[CrossRef](#)] [[PubMed](#)]
17. Vo, C.L.N.; Park, C.; Lee, B.J. Current trends and future perspectives of solid dispersions containing poorly water-soluble drugs. *Eur. J. Pharm. Biopharm.* **2013**, *85*, 799–813. [[CrossRef](#)]
18. Chatterjee, S.; Matsumoto, T.; Nishino, T.; Ooya, T. Tuned Surface and Mechanical Properties of Polymeric Film Prepared by Random Copolymers Consisting of Methacrylate-POSS and 2-(Methacryloyloxy)ethyl Phosphorylcholine. *Macromol. Chem. Phys.* **2018**, *219*, 1700572. [[CrossRef](#)]
19. Chatterjee, S.; Ooya, T. Hydrophobic Nature of Methacrylate-POSS in Combination with 2-(Methacryloyloxy)ethyl Phosphorylcholine for Enhanced Solubility and Controlled Release of Paclitaxel. *Langmuir* **2018**, *35*, 1404–1412. [[CrossRef](#)] [[PubMed](#)]
20. Liu, X.; Lei, L.; Hou, J.W.; Tang, M.F.; Guo, S.R.; Wang, Z.M.; Chen, K.M. Evaluation of two polymeric blends (EVA/PLA and EVA/PEG) as coating film materials for paclitaxel-eluting stent application. *J. Mater. Sci. Mater. Med.* **2011**, *22*, 327–337. [[CrossRef](#)]
21. Han, H.K.; Lee, B.J.; Lee, H.K. Enhanced dissolution and bioavailability of biochanin A via the preparation of solid dispersion: In vitro and in vivo evaluation. *Int. J. Pharm.* **2011**, *415*, 89–94. [[CrossRef](#)] [[PubMed](#)]
22. Chan, S.Y.; Chung, Y.Y.; Cheah, X.Z.; Tan, E.Y.L.; Quah, J. The characterization and dissolution performances of spray dried solid dispersion of ketoprofen in hydrophilic carriers. *Asian J. Pharm. Sci.* **2015**, *10*, 372–385. [[CrossRef](#)]
23. Lee, J.; Choi, J.Y.; Park, C.H. Characteristics of polymers enabling nano-comminution of water-insoluble drugs. *Int. J. Pharm.* **2008**, *355*, 328–336. [[CrossRef](#)]
24. Richard, R.E.; Schwarz, M.; Ranade, S.; Chan, A.K.; Matyjaszewski, K.; Sumerlin, B. Evaluation of acrylate-based block copolymers prepared by atom transfer radical polymerization as matrices for paclitaxel delivery from coronary stents. *Biomacromolecules* **2005**, *6*, 3410–3418. [[CrossRef](#)] [[PubMed](#)]
25. Kalogeris, I.M.; Haag Lobland, H.E. The Nature of the Glassy State: Structure and Glass Transitions. *J. Mater. Educ.* **2012**, *34*, 69–94.

26. Brostow, W.; Chiu, R.; Kalogeras, I.M.; Vassilikou-Dova, A. Prediction of glass transition temperatures: Binary blends and copolymers. *Mater. Lett.* **2008**, *62*, 3152–3155. [[CrossRef](#)]
27. Babu, R.J.; Brostow, W.; Fasina, O.; Kalogeras, I.M.; Sathigari, S.; Vassilikou-Dova, A. Encapsulation of Hydrophobic Drugs in a Copolymer: Glass Transition Behavior and Miscibility Evaluation. *Polym. Eng. Sci.* **2011**, *51*, 1456–1465. [[CrossRef](#)]
28. Tateishi, T.; Kyomoto, M.; Kakinoki, S.; Yamaoka, T.; Ishihara, K. Reduced platelets and bacteria adhesion on poly(ether ether ketone) by photoinduced and self-initiated graft polymerization of 2-methacryloyloxyethyl phosphorylcholine. *J. Biomed. Mater. Res. A* **2014**, *102*, 1342–1349. [[CrossRef](#)]
29. Que, C.L.; Gao, Y.; Raina, S.A.; Zhang, G.G.Z.; Taylor, L.S. Paclitaxel Crystal Seeds with Different Intrinsic Properties and Their Impact on Dissolution of Paclitaxel-HPMCAS Amorphous Solid Dispersions. *Cryst. Growth Des.* **2018**, *18*, 1548–1559. [[CrossRef](#)]
30. Aggarwal, A.K.; Singh, S. Physicochemical characterization and dissolution study of solid dispersions of diacerein with polyethylene glycol 6000. *Drug Dev. Ind. Pharm.* **2011**, *37*, 1181–1191. [[CrossRef](#)]
31. Miller, J.M.; Beig, A.; Carr, R.A.; Spence, J.K.; Dahan, A. A Win-Win Solution in Oral Delivery of Lipophilic Drugs: Supersaturation via Amorphous Solid Dispersions Increases Apparent Solubility without Sacrifice of Intestinal Membrane Permeability. *Mol. Pharm.* **2012**, *9*, 2009–2016. [[CrossRef](#)] [[PubMed](#)]



© 2019 by the authors. Licensee MDPI, Basel, Switzerland. This article is an open access article distributed under the terms and conditions of the Creative Commons Attribution (CC BY) license (<http://creativecommons.org/licenses/by/4.0/>).